JPE 19-1-12

https://doi.org/10.6113/JPE.2019.19.1.119
ISSN(Print): 1598-2092 / ISSN(Online): 2093-4718

Optimal Two Degrees-of-Freedom Based Neutral Point Potential Control for Three-Level Neutral Point Clamped Converters

Bo Guan† and Shinji Doki*

†School of Electrical Engineering, Chongqing University, Chongqing, China
*Department of Information and Communication Engineering, Nagoya University, Nagoya, Japan

Abstract

Although the dual modulation wave method can solve the low-frequency neutral point potential (NPP) fluctuation problem for three-level neutral point clamped converters, it also increases the switching frequency and limits the zero-sequence voltage. That makes it harmful when dealing with the NPP drift problem if the converter suffers from a long dead time or asymmetric loads. By introducing two degrees of freedom (2-DOF), an NPP control based on a search optimization method can demonstrate its ability to cope with the above mentioned two types of NPP problems. However, the amount of calculations for obtaining an optimal 2-DOF is so large that the method cannot be applied to certain industrial applications with an inexpensive digital signal processor. In this paper, a novel optimal 2-DOF-based NPP control is proposed. The relationships between the NPP and the 2-DOF are analyzed and a method for directly determining the optimal 2-DOF is also discussed. Using a direct calculation method, the amount of calculations is significantly reduced. In addition, the proposed method is able to maintain the strongest control ability for the two types of NPP problems. Finally, some experimental results are given to confirm the validity and feasibility of the proposed method.

Key words: Control ability, Direct calculation, Neutral point potential, Three level converter, Two degrees of freedom

I. INTRODUCTION

As a vital technology for medium and high voltage high power applications, multilevel converters have been widely used by scholars both nationally and abroad [1]-[3]. In particular, the three-level neutral point clamped (TL-NPC) converter is usually utilized in applications up to 10kV [3]-[5]. In this paper, some of the problems of the TL-NPC converter are discussed in detail, as shown in Fig. 1.

Although the TL-NPC converter has numerous merits when compared with two-level converters, the neutral point potential (NPP) problem should be carefully considered and solved [1]-[5]. Essentially, this problem can be classified into two types. The first type is a NPP drift problem, which originates from dead time, asymmetric loads and switching devices inconsistencies. This type of problem can damage the switching devices and DC-link capacitors [6]-[9]. The second type is a low frequency NPP fluctuation problem. This type of problem is caused by the characteristics of modulation strategies based on the nearest-three-vector pulse width modulation (NTV-PWM), such as sinusoidal PWM (SPWM), space vector PWM (SVPWM) and selective harmonic elimination PWM (SHEPWM).

In recent years, numerous methods have been developed to solve the above-mentioned two types of NPP problems. Conventional methods to solve the NPP problems are based on the SPWM or SVPWM. Since the redundant vectors in a three-level space vector diagram have opposite effects on the NPP, the authors of [6], [7] balanced the NPP by adjusting the duty cycle of the redundant vectors via a P/PI controller. Since SVPWM is equivalent to SPWM, the same NPP control performance can be realized by adjusting the zero-sequence voltage [8], [9]. Although these methods can solve

Manuscript received Jan. 9, 2018; accepted Oct. 31, 2018
Recommended for publication by Associate Editor Jaehong Kim.
†Corresponding Author: guanbo_1989@nagoya-u.jp
Tel: +86-15120074850, Chongqing University
*Dept. Informat. Commun. Eng., Nagoya University, Japan

the NPP drift problem, the generation of a low-frequency NPP fluctuation is inevitable.

It is noted in [3]-[7] that low-frequency NPP fluctuation is an important issue in NTV-PWM based NPP control. Thus, virtual space vector PWM (VSVPWM) based NPP control has been developed [10]-[15] to solve this problem. Concurrently, the authors of [16] proposed an easy method for achieving the same thing via SPWM, which is called the dual modulation wave (DMW) method. Owing to the open-loop characteristic [16] of the DMW method, some compensation methods [17] have been provided for overcoming the NPP drift problem in the VSVPWM and DMW method. However, all of these methods discuss the NPP drift problem under symmetrical loads by setting a small initial NPP drift. In addition, they do not consider the NPP control speed. Actually, the NPP control speed is an important factor for evaluating control capability for the NPP drift problem. However, the NPP control capability of the DMW method is significantly limited when compared with the conventional approaches based on NTV-PWM. The DMW method overcomes the low-frequency NPP fluctuation problem by sacrificing the control domain of the neutral point current (i_o) and maintaining i_o at zero at any time. It is harmful to deal with the NPP drift problem when the TL-NPC converter suffers from a long dead time or when it experiences asymmetrical loads. Moreover, the DMW method increases the switching frequency (SF) by 4/3 times [16], [17]. Thus, a search optimization method with two degrees of freedom (2-DOF) was proposed in [18], [19]. Here, the 2-DOF include the zero-sequence voltage (u_z) and another control variable (u_{zz}), which will be explained in detail later in Section II.C. "Optimal" implies that the selected 2-DOF are the best choices for the NPP control. Since 2-DOF can control the NPP without changing the line voltages, this method can simultaneously solve both types of NPP problems. It has an enhanced NPP control ability and can decrease the SF.

However, it has been shown in a further analysis that the calculation amount for obtaining the optimal 2-DOF is so large that the method cannot be used in some industrial applications with an inexpensive digital signal processor (DSP). Based on [18], [19], a novel optimal 2-DOF based NPP control is proposed in this paper. By analyzing the relationships between the NPP and the 2-DOF, the optimal 2-DOF can be easily acquired via an interpolation method, which can drastically reduce calculation amount. While maintaining the strongest control capability for the two types of NPP problems, the proposed method can yield the actual optimal 2-DOF instead of two quasi-optimal DOFs with the search optimization method. Moreover, the proposed method can also master the output waveforms, since the relationships between the output waveforms and the 2-DOF are clearly derived.

The remainder of this paper is organized as follows. First, Section II explains the conventional NTV-PWM based NPP control, the DMW method and the search optimization method of 2-DOF. Then, the relationships between the NPP and the 2-DOF are analyzed, and a method for achieving the optimal 2-DOF is discussed in Section III. Next, some experimental results are shown in Section IV to confirm the validity and feasibility of the proposed method. Finally, some conclusions are presented in Section V.

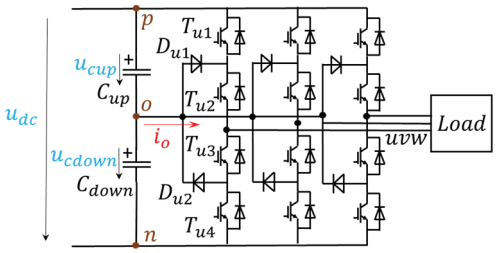

Fig. 1. TL-NPC converter (IGBTs).

II. Some Conventional NPP Control Methods and Their Disadvantages

As shown in Fig. 1, if i_o flows from a neutral point (o), the upper capacitor (C_{up}) charges and the lower capacitor (C_{down}) discharges. If i_o flows into the neutral point, C_{up} discharges and C_{down} charges [8]. Moreover, the NPP error (Δv_o) is defined as (u_{cdown}-u_{cup})/2, the relationship between i_o and Δv_o can be expressed in (1).

$$\begin{cases} C = C_{up} = C_{down} \\ i_o = -\left(2C / T_s\right)\Delta v_o \end{cases} \tag{1}$$

T_s is the control period. Therefore, it is necessary to modify the modulation modes for generating a minus neutral point current (i_{oc}) to compensate i_o, as expressed in (2) [8].

$$i_{oc} = -i_o = \left(2C / T_s\right)\Delta v_o \tag{2}$$

It is noteworthy that for different modulation modes, i_{oc} can be expressed and adjusted by different methods.

A. NTV-PWM based NPP Control

In this part, some basic principles and disadvantages of the NTV-PWM based NPP control are explained. The reference voltages (v_{ref1}, v_{ref2}) are modulated by using a space vector diagram, as displayed in Fig. 2. The reference voltage is synthesized by the nearest three vectors. Here, some redundant vectors can generate the same line voltage, but with opposite effects on i_o.

Thus, some methods [7], [8] have been developed to control the NPP by adjusting the duty time of the redundant vectors. The NPP can be controlled well when v_{ref1} is small. Meanwhile, the NPP cannot be adjusted well by the redundant vectors when v_{ref2} is large. At this point, a significant low-frequency NPP fluctuation appears when the modulation ratio (m) is big. This makes reductions of the DC-link capacitors difficult [7].

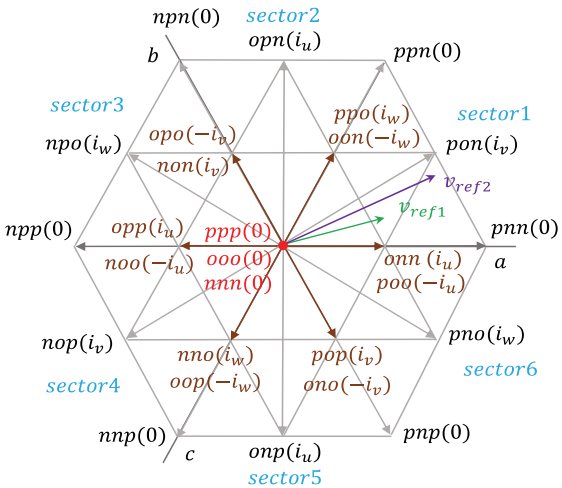

e. g. onn (i_u) means that i_o is equal to i_u for the vector onn

Fig. 2. Space vector diagram of a three level converter.

B. DMW Method based NPP Control

Given that SVPWM is equivalent to SPWM, the DMW method is illustrated here to deal with the low-frequency NPP fluctuation problem, which is a special case of VSVPWM and is easy to realize. Assume the three phase voltages (u_u, u_v, u_w) as (3).

$$\begin{cases} u_u = \left(2/\sqrt{3}\right) m\cos(\theta) \\ u_v = \left(2/\sqrt{3}\right) m\cos(\theta - 2\pi/3) \\ u_w = \left(2/\sqrt{3}\right) m\cos(\theta + 2\pi/3) \end{cases} \tag{3}$$

m is defined as $\sqrt{3}v_{ref}/u_{dc}$. A zero-sequence voltage (u_z=-(u_{max}+u_{min})/2) is injected into (u_u, u_v, u_w) to realize the maximum linear modulation, as expressed in (4). The three phase voltages with u_z injected are defined as (u_{zu}, u_{zv}, u_{zw}). Here, the maximum, middle, and minimum voltages of (u_u, u_v, u_w) are defined as (u_{max}, u_{mid}, u_{min}), and the corresponding currents of (u_{max}, u_{mid}, u_{min}) are defined as (i_{max}, i_{mid}, i_{min}).

$$\begin{cases} u_{zu} = u_u + u_z, u_{zv} = u_v + u_z, u_{zw} = u_w + u_z \\ u_z = -\left(u_{\max} + u_{\min}\right)/2 \end{cases} \tag{4}$$

The DMW method modulates the reference voltage by comparing two modulation waves with the two carrier waves ($u^p_{carrier}, u^n_{carrier}$). Thus, the two modulation waves (u_{ip}, u_{in}) are reconstructed from the reference voltage (u_{zi}), as expressed in (5).

$$\begin{cases} u_{zu} = u_{up} + u_{un} \\ u_{zv} = u_{vp} + u_{vn} \\ u_{zw} = u_{wp} + u_{wn} \end{cases} \Leftrightarrow \begin{cases} u_{zi} = u_{ip} + u_{in} \\ 0 \le u_{ip} \le 1, -1 \le u_{in} \le 0 \\ i = u, v, w \end{cases} \tag{5}$$

Consequently, the output voltage (u_{out}) can be obtained according to (6), as shown in Fig. 3. Thus, i_o can be expressed as (7) [16].

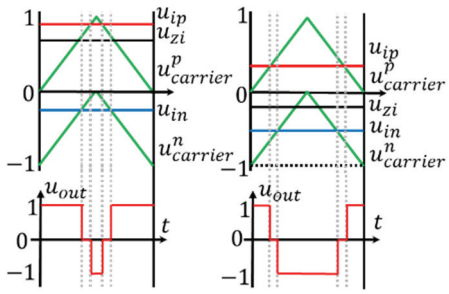

Fig. 3. DMW method: (a) $u_{zi} \ge 0$; (b) $u_{zi} < 0$.

$$u_{out} = \begin{cases} 1, if\ u_{ip} > u^p_{carrier}\ \&\&\ u_{in} > u^n_{carrier} \\ -1, if\ u_{ip} < u^p_{carrier}\ \&\&\ u_{in} < u^n_{carrier} \\ 0, if\ u_{ip} > u^p_{carrier}\ \&\&\ u_{in} < u^n_{carrier} \\ \quad or\ u_{ip} < u^p_{carrier}\ \&\&\ u_{in} > u^n_{carrier} \end{cases} \tag{6}$$

$$i_o = \left|1 + u_{un} - u_{up}\right| i_u + \left|1 + u_{vn} - u_{vp}\right| i_v + \left|1 + u_{wn} - u_{wp}\right| i_w \tag{7}$$

To overcome low-frequency NPP fluctuation, it is necessary to ensure that i_o can be maintained at zero at all times. Equation (8) exhibits a special solution (u_x=(u_{min}-u_{max})/2) of (7).

$$\begin{aligned} &if\ \left|1 + u_{un} - u_{up}\right| = \left|1 + u_{vn} - u_{vp}\right| = \left|1 + u_{wn} - u_{wp}\right| = \left|1 + u_x\right| \\ &then\ i_o = \left|1 + u_x\right|\left(i_u + i_v + i_w\right) = 0 \end{aligned} \tag{8}$$

Then the reconstructed modulation waves (u_{ip}, u_{in}) can be rewritten in (9) [16].

$$\begin{cases} u_{ip} = \dfrac{u_i - u_{\min}}{2} \ge 0 \\ u_{in} = \dfrac{u_i - u_{\max}}{2} \le 0 \end{cases}, \quad i = u, v, w \tag{9}$$

It can be seen from (6) and (9) that when the reference voltage is equal to u_{mid}, the PWM waveforms of u_{out} are similar to the waveforms in Fig. 3 [17]. Since two switching transforms occur during a control period, the SF of the DMW method is 1/3 larger than that of the NTV-PWM.

C. NPP Control based on the Search Optimization Method of 2-DOF

Although the DMW method can solve the low-frequency NPP fluctuation problem, it is simply an open-loop method, which has difficulty dealing with the NPP drift problem. Some methods [17] were developed to compensate for the NPP drift. However, the DMW method essentially sacrifices many control domains of i_o to keep i_o at zero, when compared with NTV-PWM. It limits the control capability for coping with a serious NPP drift problem when a system is suffering from a long dead time or experiencing strong asymmetrical loads. Therefore, the control domains of i_o under the NTV-PWM and DMW methods with a compensator are given here in Fig. 4 at different values for both m and the power factor angle (φ). The

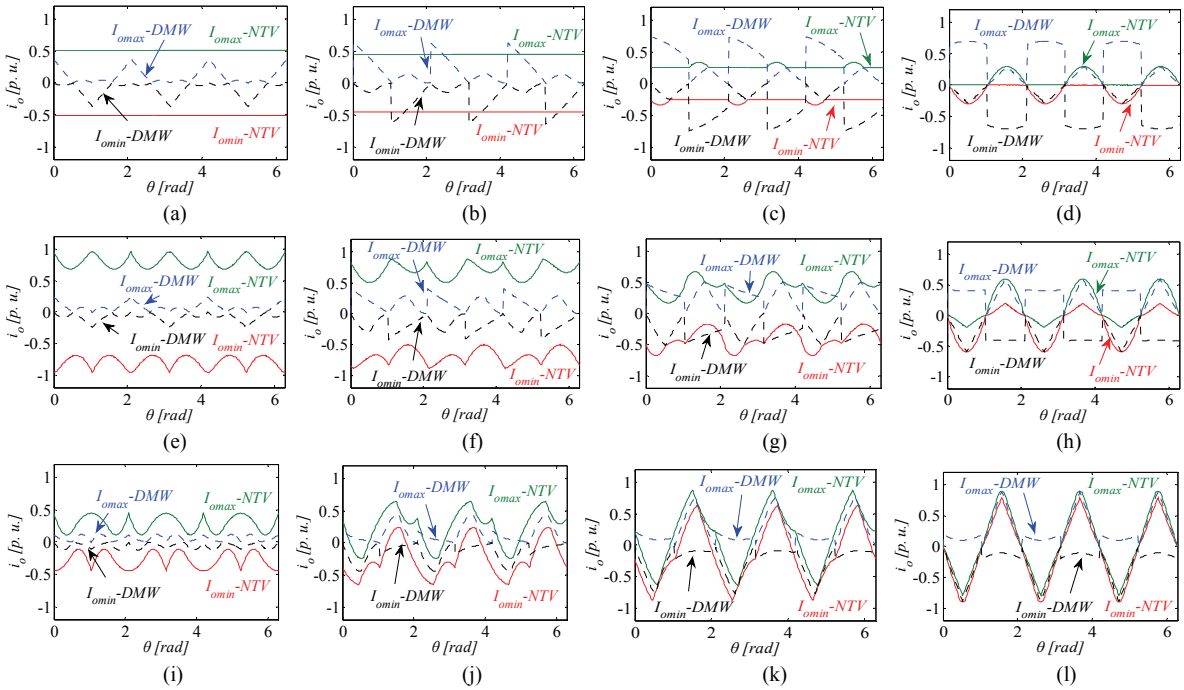

Fig. 4. Control domains of i_o under the NTV-PWM and DMW methods: (a) φ=0, m=0.3; (b) φ=π/6, m=0.3; (c) φ=π/3, m=0.3; (d) φ=π/2, m=0.3; (e) φ=0, m=0.6; (f) φ=π/6, m=0.6; (g) φ=π/3, m=0.6; (h) φ=π/2, m=0.6; (i) φ=0, m=0.9; (j) φ=π/6, m=0.9; (k) φ=π/3, m=0.9; (l) φ=π/2, m=0.9.

results at different values of m and φ are provided to demonstrate the generality of the analysis and discussion. In Fig. 4, the horizontal axis represents the phase angle (θ) of the reference voltage of phase u. The vertical axis shows the adjustment range of i_o. The NTV-PWM and DMW methods can be used to adjust i_o from I_{omax} to I_{omin}. Thus, the difference between I_{omax} and I_{omin} determines control capability for compensating i_{oc}. Thus, the method that has a wider control domain for i_o has a stronger control ability for the NPP drift problem.

Under ideal operation conditions, it is necessary to keep i_o zero during the entire region of θ, since it is directly related to the low-frequency NPP fluctuation. For example, it can be found in Figs. 4(a-g) and (i) that I_{omax}-*NTV* is always larger than zero and that I_{omin}-*NTV* is smaller than zero. Therefore, i_o can be adjusted to zero by amending u_z. This does not result in the low frequency NPP fluctuation problem under these operation conditions for NTV-PWM. However, it can be seen from Figs. 4(h) and (j-l) that both I_{omax}-*NTV* and I_{omin}-*NTV* may be simultaneously larger or smaller than zero for some θ. Therefore, it is not possible to keep i_o at zero during the whole period. A low-frequency NPP fluctuation is generated under these operation conditions.

However, it is easy to see from Fig. 4 that I_{omax}-*DMW* is always larger than zero, whereas I_{omin}-*DMW* is smaller than zero under all operation conditions. Thus, it is possible to keep i_o zero to completely avoid the low frequency NPP fluctuation problem. However, it can be seen that the control domain of i_o for the DMW method with a compensator

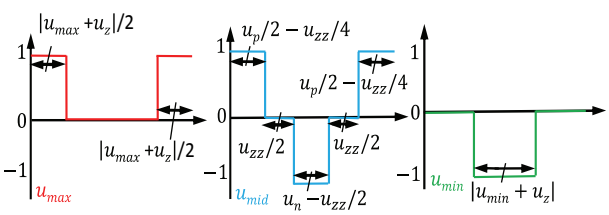

Fig. 5. PWM waveforms of the proposed method.

sometimes becomes narrower than that in the NTV-PWM, as shown in Figs. 4 (a), (b), (e), (f) and (j). Therefore, as mentioned above, although the DMW method can overcome the low frequency NPP fluctuation problem that exists in NTV-PWM under some operation conditions, the control capability for the NPP drift problem is weakened and the control speed for the NPP drift problem is slowed down.

The search optimization method in [18], [19] introduces 2-DOF (u_z, u_{zz}) to solve the two types of NPP problems. This method has a stronger control capability for the NPP drift problem. The first DOF is the zero-sequence voltage (u_z). It is possible to control the NPP by adjusting u_z within a limit range, as given in (10). This is similar to the conventional NTV-PWM based NPP control.

$$-1-u_{\min} \le u_z \le 1-u_{\max} \tag{10}$$

Simultaneously, the duty time of the voltage (0) is defined as another DOF (u_{zz}), as shown in Fig. 5. A special modulation mode is performed in u_{mid}. Here, the duty times (u_p, u_n) are calculated in (11).

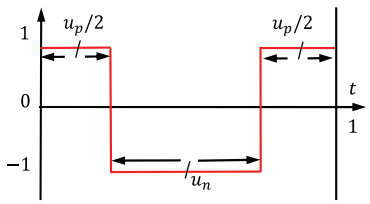

Fig. 6. Extreme case one.

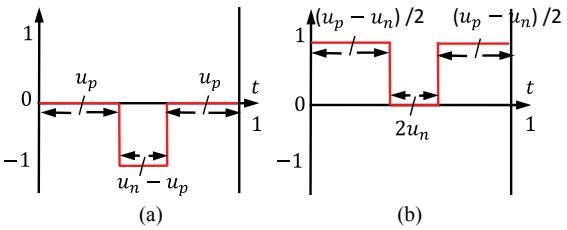

Fig. 7. Extreme case two: (a) $u_p<u_n$; (b) $u_p>u_n$.

$$\begin{cases} u_p = (1 + u_{mid} + u_z)/2 \\ u_n = (1 - u_{mid} - u_z)/2 \end{cases} \tag{11}$$

Thus, it is very important to decide the limit range of u_{zz}. Two extreme cases are obtained, which can be utilized to determine the limit range of u_{zz}. The first extreme case is depicted in Fig. 6. It can be seen from Fig. 6 that u_{zz} decreases to 0, as shown in (12). Moreover, the three-level modulation is degraded to a two-level modulation. This is undesirable, since it may result in the loss of some of the advantages of a three-level converter. For example, it is harmful for the electromagnetic interference (EMI) problem.

$$0 \le u_{zz} \tag{12}$$

The other extreme case is presented in Fig. 7. Then the limit range of u_{zz} can be fixed as (13).

$$u_{zz} \le 2\min(u_p, u_n) \tag{13}$$

It can be seen from Fig. 7 that the output waveforms become similar to the NTV-PWM method instead of the DMW method. This is key to reducing the SF for high-power applications. More importantly, the boundaries of the NTV-PWM and DMW methods are blurred. Transitions between two modulation modes is performed based on the NPP control.

Lastly, the limit range of u_{zz} can be expressed as (14).

$$0 \le u_{zz} \le 2\min(u_p, u_n) \tag{14}$$

Concurrently, i_o, which is caused by u_z and u_{zz}, can be expressed in (15) based on Fig. 5.

$$\begin{aligned} & i_o = i_{\max o} + i_{\min o} + i_{mido} \\ & \begin{cases} i_{\max o} = (1 - |u_{\max} + u_z|) i_{\max} \\ i_{\min o} = (1 - |u_{\min} + u_z|) i_{\min} \\ i_{mido} = u_{zz} i_{mid} \end{cases} \end{aligned} \tag{15}$$

From (2), (10), (14) and (15), it is known that it is necessary to adjust u_z and u_{zz} to meet the following equation:

$$\Delta v_o = -\frac{(1 - |u_{\max} + u_z|) i_{\max} + (1 - |u_{\min} + u_z|) i_{\max} + u_{zz} i_{mid}}{(2C / T_s)} \tag{16}$$

However, it is difficult to obtain the optimal u_z and u_{zz} from (16), particularly when the limit range of u_{zz} is governed by u_z. As a simple approach, the search optimization method of 2-DOF is proposed in [18], [19]. All of the values of u_z and u_{zz} are searched within the limit ranges of (10) and (14) and then Δv_{oc} is calculated. Next, the optimal values of u_z and u_{zz}, for which Δv_{oc} is closest to Δv_o, are chosen. Lastly, to unify the modulation modes as (6), three phase voltages are reconstructed in (17). The *floor* in (17) implies a floor function.

$$\begin{aligned} & \begin{cases} u_{\max p} = (u_{\max} + u_z) \cdot [1 + \text{floor}(u_{\max} + u_z)] \\ u_{\max n} = -(u_{\max} + u_z) \cdot \text{floor}(u_{\max} + u_z) \end{cases} \\ & \begin{cases} u_{\min p} = (u_{\min} + u_z) \cdot [1 + \text{floor}(u_{\min} + u_z)] \\ u_{\min n} = -(u_{\min} + u_z) \cdot \text{floor}(u_{\min} + u_z) \end{cases} \\ & u_{midp} = u_p - u_{zz}/2, u_{midn} = -(u_n - u_{zz}/2) \end{aligned} \tag{17}$$

Thus, when the optimal values of u_z and u_{zz} are achieved, the reference voltages can be easily modulated based on (6) and (17). Similarly, the control domains of i_o for the DMW method and the search optimization method of 2-DOF can be analyzed in Fig. 8 at different values of m and φ. Firstly, it can be seen from Fig. 8 that I_{omax}-*2DOF* is always larger than zero, and that I_{omin}-*2DOF* is smaller than zero under all the operation conditions. Thus, the search optimization method of 2-DOF can also solve the low-frequency NPP fluctuation problem. Furthermore, when compared with the NTV-PWM and DMW methods, it can be seen that the control domain of i_o for the search optimization method of 2-DOF is typically the widest under all the operation conditions. The search optimization method of 2-DOF can deal with a more serious NPP drift problem and it can enhance the control speed when the system is suffering from a long dead time, strong asymmetrical loads and so on. When compared with the DMW method, the search optimization method of 2-DOF does not sacrifice any advantages, and achieves a stronger NPP control capability.

III. Optimal 2-DOF Based NPP Control for TL-NPC Converters

As analyzed in Section II and in [18], [19], it can be found that the search optimization method can simultaneously solve the NPP drift problem and the low frequency NPP fluctuation problem. Concurrently, it can achieve the widest control domain of i_o and reduce the SF by mastering the 2-DOF. The method is a good choice for reducing DC-link capacitors, which is very important for reducing the weight and volume of TL-NPC converters. However, the problem is that the

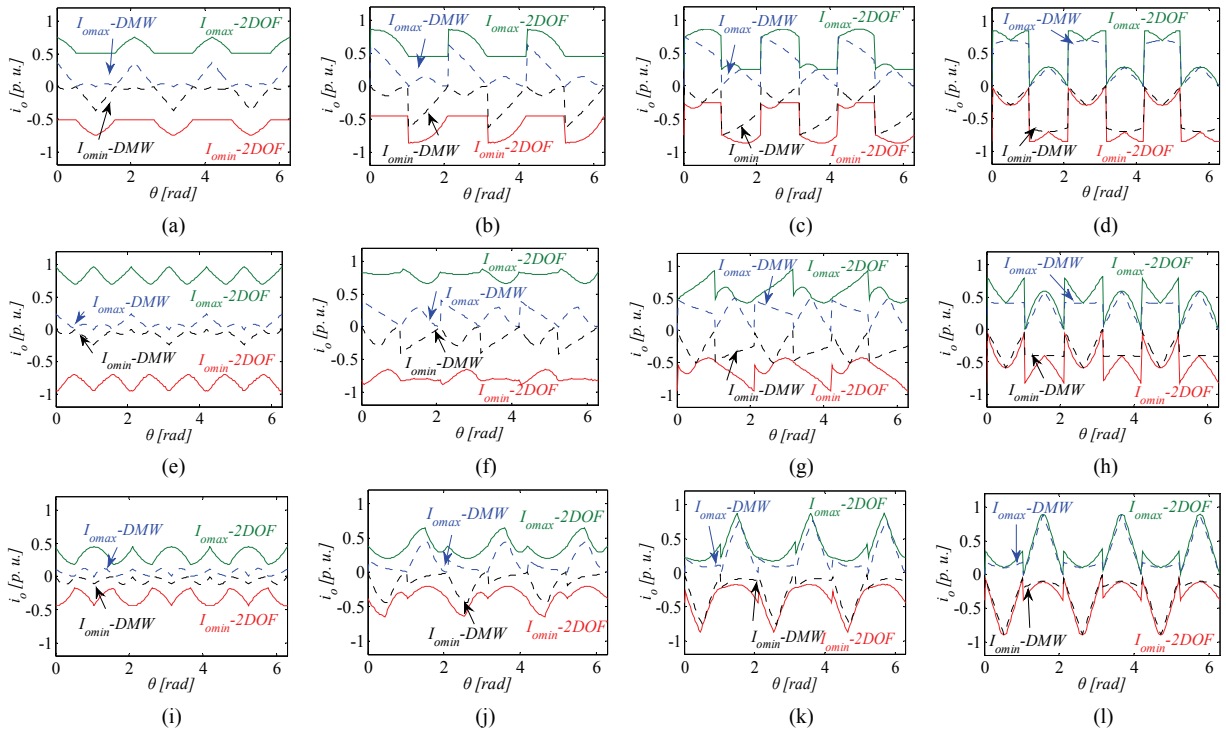

Fig. 8. Control domains of i_o under the DMW method and the search optimization method of 2-DOF: (a) φ=0, m=0.3; (b) φ=π/6, m=0.3; (c) φ=π/3, m=0.3; (d) φ=π/2, m=0.3; (e) φ=0, m=0.6; (f) φ=π/6, m=0.6; (g) φ=π/3, m=0.6; (h) φ=π/2, m=0.6; (i) φ=0, m=0.9; (j) φ=π/6, m=0.9; (k) φ=π/3, m=0.9; (l) φ=π/2, m=0.9.

amount of calculations for obtaining the optimal 2-DOF is so large that the method cannot be adopted in some industrial applications with an inexpensive DSP. For example, if both u_z and u_{zz} are divided into 1000 parts each, it is necessary to predict Δv_{oc} by 10^6 times to obtain the optimal u_z and u_{zz}. Moreover, the 2-DOF are simply quasi-optimal in principle. Therefore, a direct calculation method with a small calculation amount is necessary in some applications with an inexpensive DSP.

In this paper, a novel optimal 2-DOF based NPP control for TL-NPC converters is proposed. The proposed method can simultaneously solve the NPP drift problem and the low frequency NPP fluctuation problem. Concurrently, it has a strong control capability and a fast control speed for the NPP drift problem. More importantly, the proposed method can reach the objective with a small amount of calculations, which can be burdened by an inexpensive DSP. Instead of a quasi-optimal result, the proposed method can yield the actual optimal 2-DOF.

A. Relationships between i_o, u_z and u_{zz}

In this part, the relationships between i_o, u_z and u_{zz} are directly analyzed in detail to obtain a direct calculation method for the optimal u_z and u_{zz}. First, i_o in the search optimization method in section II and in [18], [19] can be rewritten as (18).

$$\begin{cases} i_o = -\sum\limits_{i=\min,mid,\max} |u_i + u_z| i_i - k u_{zz\max} i_{mid} \\ u_{zz\max} = \min\left(1+u_{mid}+u_z, 1-u_{mid}-u_z\right) = 1-|u_{mid}+u_z| \end{cases} \tag{18}$$

Then, i_o can also be expressed in (19).

$$\begin{aligned} i_o &= -|u_{\max}+u_z| i_{\max} - |u_{mid}+u_z| i_{mid} \\ &\quad - |u_{\min}+u_z| i_{\min} - k\left(1-|u_{mid}+u_z|\right) i_{mid} \\ &= -|u_{\max}+u_z| i_{\max} - |u_{\min}+u_z| i_{\min} \\ &\quad - (1-k)|u_{mid}+u_z| i_{mid} - k i_{mid} \end{aligned} \tag{19}$$

Based on the sign of the absolute parts in (19), i_o is classified into four cases.

1) If -1-u_{min}<u_z<-u_{max}, (19) can be rewritten as:

$$\begin{aligned} i_o &= (u_{\max}+u_z) i_{\max} + (u_{\min}+u_z) i_{\min} + (1-k)(u_{mid}+u_z) i_{mid} - k i_{mid} \\ &= u_{\max} i_{\max} + u_{\min} i_{\min} + u_{mid} i_{mid} - k(u_{mid}+u_z) i_{mid} - k i_{mid} \\ &= c_1 - k(1+u_{mid}+u_z) i_{mid} \end{aligned} \tag{20}$$

2) If -u_{max}<u_z<-u_{mid}, (19) can be rewritten as:

$$\begin{aligned} i_o &= -(u_{\max}+u_z) i_{\max} + (u_{\min}+u_z) i_{\min} + (1-k)(u_{mid}+u_z) i_{mid} - k i_{mid} \\ &= -u_{\max} i_{\max} + u_{\min} i_{\min} + u_{mid} i_{mid} - 2u_z i_{\max} - k(u_{mid}+u_z) i_{mid} - k i_{mid} \\ &= c_2 - 2u_z i_{\max} - k(1+u_{mid}+u_z) i_{mid} \end{aligned} \tag{21}$$

3) If -u_{mid}<u_z<-u_{min}, (19) can be rewritten as:

$$\begin{aligned} i_o &= -(u_{\max}+u_z) i_{\max} + (u_{\min}+u_z) i_{\min} - (1-k)(u_{mid}+u_z) i_{mid} - k i_{mid} \\ &= -u_{\max} i_{\max} + u_{\min} i_{\min} - u_{mid} i_{mid} + 2u_z i_{\min} + k(u_{mid}+u_z) i_{mid} - k i_{mid} \\ &= c_3 + 2u_z i_{\min} - k(1-u_{mid}-u_z) i_{mid} \end{aligned} \tag{22}$$

4) If -u_{min}<u_z<1-u_{max}, (19) can be rewritten as:

$$\begin{aligned} i_o &= -(u_{\max}+u_z)i_{\max} - (u_{\min}+u_z)i_{\min} - (1-k)(u_{mid}+u_z)i_{mid} - ki_{mid} \\ &= -u_{\max}i_{\max} - u_{\min}i_{\min} - u_{mid}i_{mid} - k(u_{mid}+u_z)i_{mid} - ki_{mid} \\ &= c_4 - k(1-u_{mid}-u_z)i_{mid} \end{aligned} \tag{23}$$

Here, c_1-c_4 are intermediate variables. k is used to control u_{zz}. i_o is simultaneously adjusted by u_z and k. If k is equal to 0, it implies that u_{zz} is not used to control i_o, and the modulation mode returns to NTV-PWM. This is good for reducing the SF. The neutral point current (i_{zo}) when k is equal to 0, can be expressed as follows:

1) If -1-u_{min}<u_z<-u_{max}, then i_o can be rewritten as:

$$\begin{cases} i_{zo} = u_{\max}i_{\max} + u_{\min}i_{\min} + u_{mid}i_{mid} = c_1 \\ i_{zo}(p0) = i_{zo}(-1-u_{\min}) = c_1 \\ i_{zo}(p1) = i_{zo}(-u_{\max}) = c_1 \end{cases} \tag{24}$$

2) If -u_{max}<u_z<-u_{mid}, then i_o can be rewritten as:

$$\begin{cases} i_{zo} = -u_{\max}i_{\max} + u_{\min}i_{\min} + u_{mid}i_{mid} - 2u_z i_{\max} = c_2 - 2u_z i_{\max} \\ i_{zo}(p2) = i_{zo}(-u_{mid}) \\ = -u_{\max}i_{\max} + u_{\min}i_{\min} + u_{mid}i_{mid} + 2u_{mid}i_{\max} = c_2 + 2u_{mid}i_{\max} \end{cases} \tag{25}$$

3) If -u_{mid}<u_z<-u_{min}, then i_o can be rewritten as:

$$\begin{cases} i_{zo} = -u_{\max}i_{\max} + u_{\min}i_{\min} - u_{mid}i_{mid} + 2u_z i_{\min} = c_3 + 2u_z i_{\min} \\ i_{zo}(p3) = i_{zo}(-u_{\min}) \\ = -u_{\max}i_{\max} + u_{\min}i_{\min} - u_{mid}i_{mid} - 2u_{\min}i_{\min} = c_4 \end{cases} \tag{26}$$

4) If -u_{min}<u_z<1-u_{max}, then i_o can be rewritten as:

$$\begin{cases} i_{zo} = -u_{\max}i_{\max} - u_{\min}i_{\min} - u_{mid}i_{mid} = c_4 \\ i_{zo}(p4) = i_{zo}(1-u_{\max}) = c_4 \end{cases} \tag{27}$$

On the other hand, if k is equal to 1, this implies that u_{zz} is fully utilized. Thus, the neutral point current (i_{zzo}) when k is equal to 1, can be expressed as follows.

1) If -1-u_{min}<u_z<-u_{max}, then i_o can be rewritten as:

$$\begin{cases} i_{zzo} = c_1 - (1+u_{mid}+u_z)i_{mid} \\ i_{zzo}(p0) = i_{zo}(p0) - (u_{mid}-u_{\min})i_{mid} \\ i_{zzo}(p1) = i_{zo}(p1) - (1+u_{mid}-u_{\max})i_{mid} \end{cases} \tag{28}$$

2) If -u_{max}<u_z<-u_{mid}, then i_o can be rewritten as:

$$i_{zzo}(p2) = i_{zo}(p2) - i_{mid} \tag{29}$$

3) If -u_{mid}<u_z<-u_{min}, then i_o can be rewritten as:

$$i_{zzo}(p3) = i_{zo}(p3) - (1-u_{mid}+u_{\min})i_{mid} \tag{30}$$

4) If -u_{min}<u_z<1-u_{max}, then i_o can be rewritten as:

$$i_{zzo}(p4) = i_{zo}(p4) - (-u_{mid}+u_{\max})i_{mid} \tag{31}$$

However, *p0-p4* cannot be obtained simultaneously under some operation conditions.

1) If u_{max}-u_{min}<1, then the points (*p0-p4*) can be obtained.
2) If u_{max}-u_{min}>1, then the points (*p1*, *p3*) cannot be obtained.

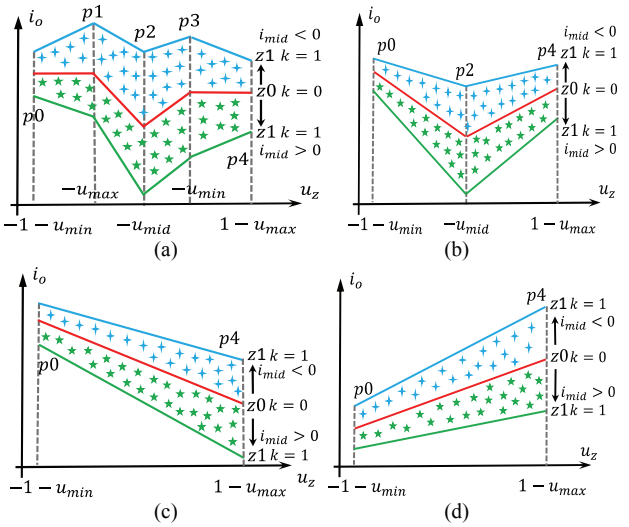

Fig. 9. Relationships between i_o, u_z and k: (a) u_{max}-u_{min}<1; (b) u_{max}-u_{min}>1 and $|u_{mid}|$+max($|u_i|$)<1; (c) u_{max}-u_{min}>1 and u_{max}-u_{mid}>1; (d) u_{max}-u_{min}>1 and u_{mid}-u_{min}>1

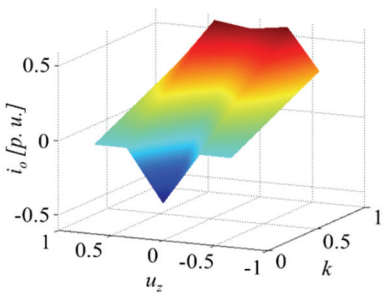

Fig. 10. 3-D diagram of the relationships between i_o, u_z and k.

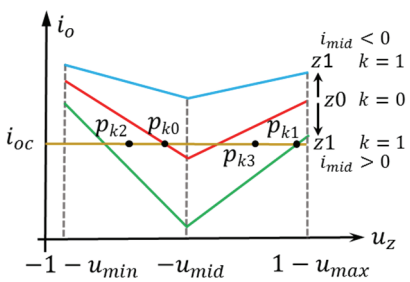

Fig. 11. Example of determining the optimal values for u_z and k.

3) If $|u_{mid}|$+max($|u_i|$)>1, the points (*p1*, *p2*, *p3*) cannot be achieved.

Therefore, the tracks of i_o can be drawn into the four cases in Fig. 9. The three-dimensional diagram is shown in Fig. 10.

B. Control Flow to Achieve the Optimal 2-DOF

For example, if Δv_o exists, which needs to be compensated by i_{oc} in Fig. 11, it is necessary to consider how to determine the optimal values for u_z and k. It is noted from Fig. 11 that there are numerous choices for generating the same i_{oc}. The NPP control proposed in section III searches for all of the points in Fig. 10 to determine u_z and k. The chosen u_z and k

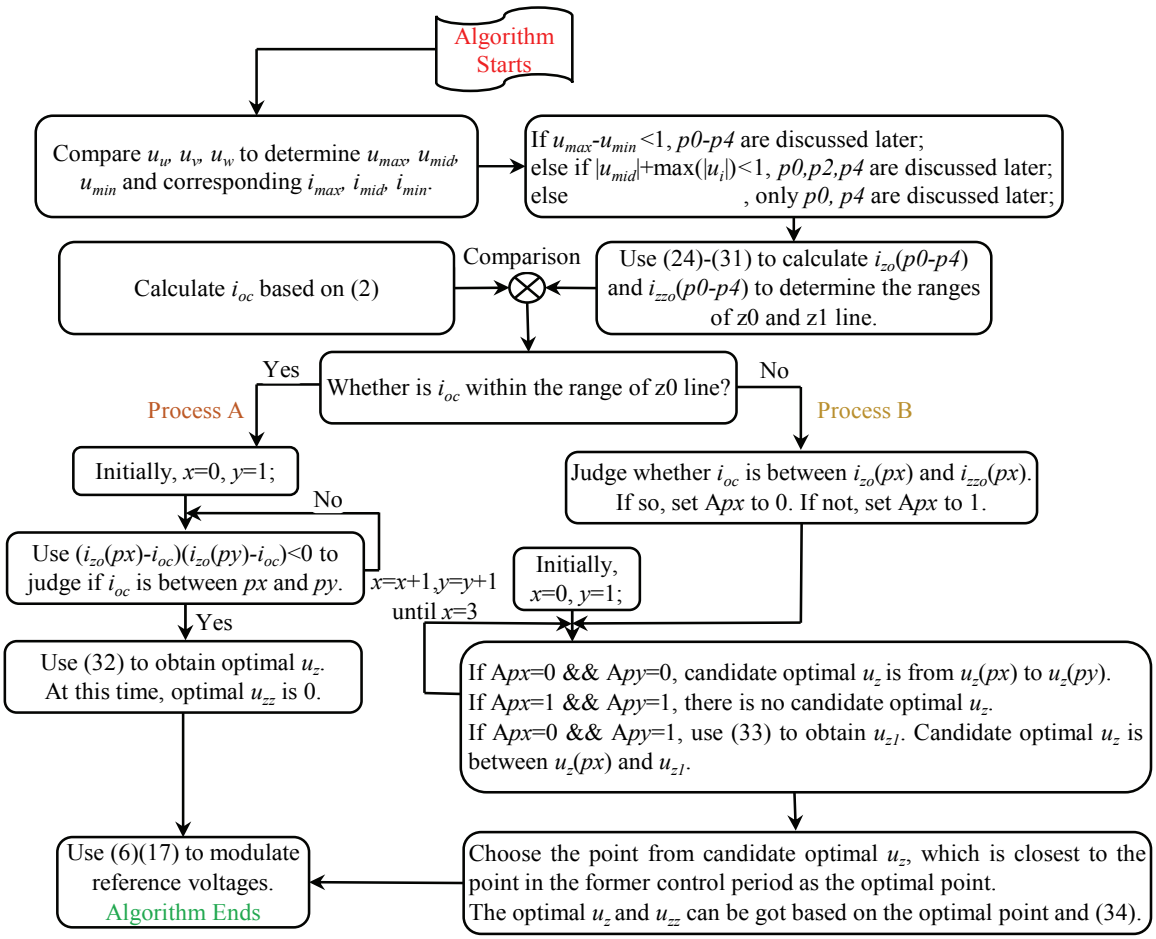

Fig. 12. Overall flow chart of the proposed direct calculation method.

correspond to the last point that can generate the required i_{oc}. In Fig. 11, the point (p_{k1}) is chosen. It needs a large amount of calculations and causes the three-level modulation to degrade to a two-level modulation. Furthermore, different choices correspond to different output performances. For example, if the point (p_{k0}) is chosen, the modulation mode returns to NTV-PWM, which is beneficial for improving the SF. If the point (p_{k2}) is chosen in the former control period and the point (p_{k3}) is chosen in this control period, it causes an additional switching. Moreover, the harmonic characteristics are also different for different points.

Because NTV-PWM has some advantages in terms of the SF and harmonic characteristics, the point on z0 line is chosen preferentially. For example, in Fig. 11, although the points (p_{k0}-p_{k3}) can generate the same i_{oc}, the point (p_{k0}) is chosen. The optimal u_z and k are decided as follows.

1) Compare three phase voltages to determine the maximum, middle and minimum voltages (u_{max}, u_{mid}, u_{min}) and their corresponding currents (i_{max}, i_{mid}, i_{min}).

2) Use the voltage limits (u_{max}-u_{min}<1, $|u_{mid}|$+max($|u_i|$)<1) to determine the tracks of i_o, as shown in Fig. 9.

3) Calculate i_{zo}(p0-p4) and i_{zzo}(p0-p4) to determine the ranges of the z0 and z1 lines.

4) Calculate i_{oc} and decide which zone i_{oc} is in to try different processes, A or B.

Process A: (i_{oc} is within the range of the z0 line).

a1) Use (i_{zo}(px)-i_{oc})(i_{zo}(py)-i_{oc})<0 to judge if i_{oc} is between the points px and py (x, y = 0, 1 , 2, 3, 4).

a2) If i_{oc} is between px and py, an interpolation theory is used [9] to obtain the optimal u_z as (32). At this time, the optimal k is equal to 0. This is to say, u_{zz} is 0.

$$u_z = \frac{u_z(py)\left[i_{oc} - i_{zo}(px)\right] - u_z(px)\left[i_{oc} - i_{zo}(py)\right]}{i_{zo}(py) - i_{zo}(px)} \quad (32)$$

Process B: (i_{oc} is beyond the range of the z0 line).

b1) Judge whether i_{oc} is between i_{zo}(px) and i_{zzo}(px). If it is, set Apx to 0. If it is not, set Apx to 1.

b2) If Apx and Apy are both 0, all of the u_z between u_z(px) and u_z(py) are candidates for the optimal u_z. If Apx and Apy are both 1, there is no candidate for an optimal u_z between u_z(px) and u_z(py). If Apx is 0 and Apy is 1, the interpolation theory can be used to obtain one optimal u_{z1} as (33). At this time, the candidate optimal u_z is between u_z(px) and u_{z1}.

$$u_{z1} = \frac{u_z(py)\left[i_{oc} - i_{zzo}(px)\right] - u_z(px)\left[i_{oc} - i_{zzo}(py)\right]}{i_{zzo}(py) - i_{zzo}(px)} \quad (33)$$

b3) Because all of the candidates for the optimal u_z have been obtained, u_{zz} is determined as in (34).

$$u_{zz} = -\frac{i_{oc} - \sum_{i=\max,mid,\min} \left(1-\left|u_i + u_z\right|\right) i_i}{i_{mid}} \tag{34}$$

b4) Last, the final optimal u_z and u_{zz} should be decided, considering the SF. If the point (*pa*) is chosen in the former control period, the point that is closest to *pa* is chosen as the final optimal point in this control period. Then the optimal values for u_z and u_{zz} can also be determined based on the final optimal point.

An overall flow chart is shown in Fig. 12.

IV. Experimental Verification

In this section, some experimental results are presented to verify the advantages of the proposed method when compared with the conventional NPP controls. The experiment set-up is based on a DSP/TMS320C 6657 and a FPGA/XC6SLX45, as displayed in Fig. 13. The TL-NPC converter is composed of a three-phase diode rectifier and a three-phase TL-NPC inverter. The current sensor board and voltage sensor board are based on a LEM/FA-050P and a LEM/LV-25P, respectively. Moreover, a voltage slider is utilized to adjust the DC-link voltage to 220 V. The parameters are listed in Table I. Because the NPP control performance of the proposed method only depends on m and the power factor (PF) in principle, the output frequency can be set to any value. However, do to limitations in the experimental environment, it is set to 40Hz for obtaining the loads, where the PF is approximately 0.37, 0.625 and 0.99.

A. NPP Control Performance of the Proposed Method in Stable Loads

In this part, five sets of experimental results under different operation conditions are presented to discuss the four methods. The operation conditions are shown as follows.

1) Operation condition 1 (OC1):
   R1-L1(5Ω/25mH) PF = 0.625, m = 0.85
2) Operation condition 2 (OC2):
   R1-L1(5Ω/25mH) PF = 0.625, m = 0.75
3) Operation condition 3 (OC3):
   R2-L2(2.5Ω/25mH) PF = 0.37, m = 0.85
4) Operation condition 4 (OC4):
   R2-L2(2.5Ω/25mH) PF = 0.37, m = 0.75
5) Operation condition 5 (OC5):
   R3-L3(10Ω/5mH) PF = 0.99, m = 0.85

The initial NPP error (Δv_o) is set as 30V. The experimental results of these methods are shown in Figs. 14-17, Figs. 18-21, Figs. 22-24, Figs. 25-27 and Fig. 28 for OC1-5. A lot of results are given here to confirm the validity and feasibility of the proposed method under any operation condition. Because the results under all of the operation conditions provide similar conclusions, a detailed description of Figs. 14-17 is given.

TABLE I
Experimental Parameters

Items	Parameters
DC-link voltage	220 V
Cup and Cdown	1800 uF
Switching frequency	4 kHz
Output frequency (f_s)	40 Hz
Loads	R1-L1(5Ω/25mH) PF=0.625 R2-L2(2.5Ω/25mH) PF=0.37 R3-L3(10Ω/5mH) PF=0.992

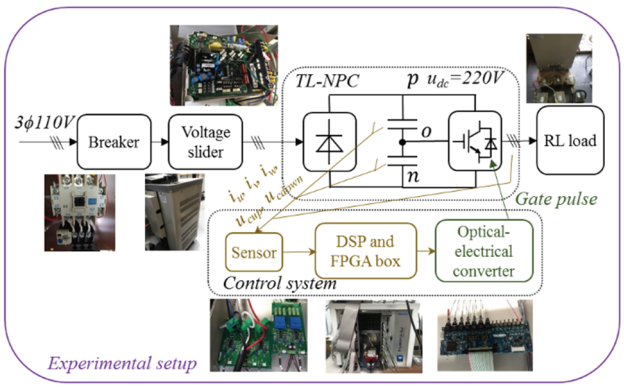

Fig. 13. Experimental setup.

Figs. 14 and 15 show experimental results of the NTV-PWM based NPP control and the DMW method with a compensator. First, it is known from Fig. 14(c) that the NPP drift can be controlled to 0 within 40 ms. However, a low frequency fluctuation appears in the NPP, which limits the reductions of the capacitors. Concurrently, the SF of the conventional NPP control is 4 kHz and the calculation time (CT) is approximately 3 us for a TMS320C6657, as shown in Fig. 14(d). However, as shown in Fig. 15(c), both the NPP drift and the low frequency NPP fluctuation are solved with the DMW method. The problem is that the SF increases to 5.3 kHz. In addition, the three-level modulation sometimes degrades to a two-level modulation, as shown in Figs. 14(a) and 15(a). A two-level converter should generate $-u_{dc}/2$ and $u_{dc}/2$. A three-level converter should generate $-u_{dc}/2$, 0 and $u_{dc}/2$. Therefore, the condition that a method can generate a voltage (0) determines whether a method is a two-level or three-level modulation. However, it can be seen from Fig. 15(a) that when the output voltage changes from -100 V to 100 V, the conventional DMW method with a compensator cannot generate a voltage (0). Therefore, for the conventional DMW method, the three-level modulation will be degraded to a two-level modulation. This is undesirable, since some of the advantages of three-level converters disappear. For example, the du/dt increases, which is harmful for improving the EMI. From Fig. 14(b) and 15(b), it is also noted that the range of u_z for NTV-PWM is wider than that for the DMW method.

Experimental results of the search optimization method of 2-DOF are given, as shown in Fig. 16. It can be seen from Fig. 16(b) that the 2-DOF (u_z and u_{zz}) are adjusted in a wider

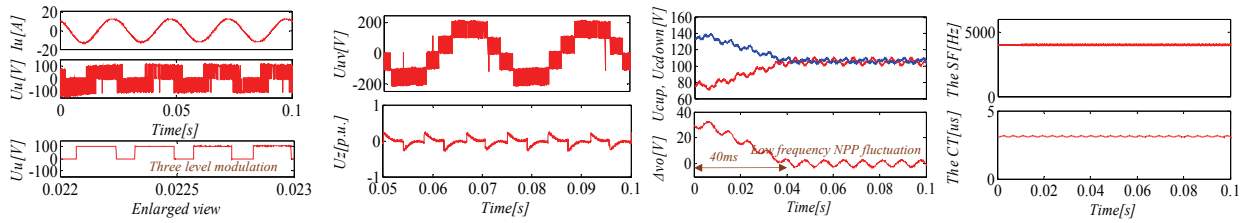

(a) (b) (c) (d)

Fig. 14. Conventional NTV-PWM based NPP control (OC1): (a) i_u and u_u; (b) u_{uv} and u_z; (c) *NPP*; (d) SF and CT.

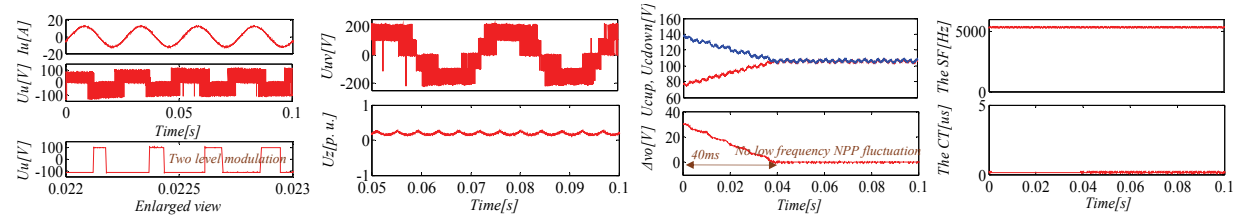

(a) (b) (c) (d)

Fig. 15. Conventional DMW method with a compensator (OC1): (a) i_u and u_u; (b) u_{uv} and u_z; (c) *NPP*; (d) SF and CT.

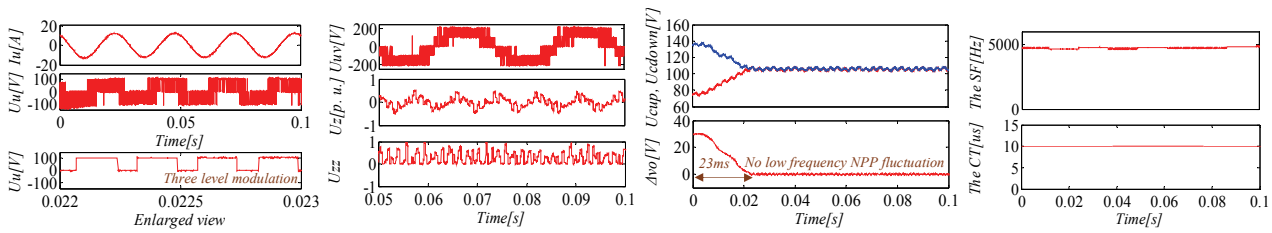

(a) (b) (c) (d)

Fig. 16. NPP control based on the search optimization method of 2-DOF (OC1): (a) i_u and u_u; (b) u_{uv}, u_z and u_{zz}; (c) *NPP*; (d) SF and CT.

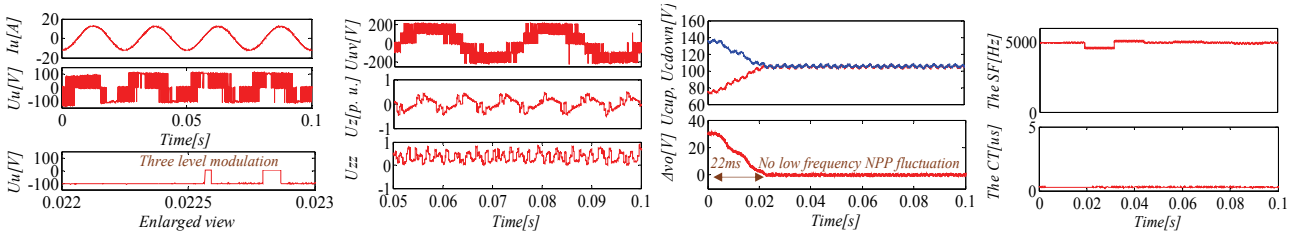

(a) (b) (c) (d)

Fig. 17. Proposed direct calculation method of the optimal 2-DOF based NPP control (OC1): (a) i_u and u_u; (b) u_{uv}, u_z and u_{zz}; (c) *NPP*; (d) SF and CT.

range. Moreover, this method can avoid the degradation of the three- level modulation to a two-level modulation when compared with the DMW method, as shown in Figs. 15(a) and 16(a). Concurrently, the NPP drift and low-frequency NPP fluctuation problems can also be solved simultaneously. Moreover, it is noteworthy that the control speed of the NPP drift problem is faster at 20 ms. This corresponds to a stronger NPP control capability for the NPP drift problem, which is generated from a long dead time or strong asymmetric loads. Furthermore, the SF is also decreased from 5.3 kHz to 4.8 kHz. However, as analyzed in Section III, the CT increases to approximately 10 us. Here, u_z and u_{zz} are divided into 100 parts and 10 part, respectively. If a more accurate control is desired, the CT becomes larger than 10 us, which is intolerant for some inexpensive DSPs and applications.

The direct calculation method can realize the same control performance as the search optimization method with a lower amount of calculations. Experimental results of the proposed method are shown in Figs. 17 and 18 at different loads. It can be seen from Fig. 17(c) that the NPP drift and low frequency NPP fluctuation problems have been overcome within 22 ms. From Fig. 17(d), it is known that the CT is reduced from 10 us to 0.3 us. This ensures that the three-level modulation does not degrade to a two-level modulation.

Simultaneously, FFT analyses of the line voltage and characteristics of the four methods are summarized in Table II under OC1. According to the THD and SF in Table II, the conventional NPP control has the best output performance, since it adopts NTV-PWM. However, the NPP drift control ability is in the middle and the low-frequency NPP fluctuation

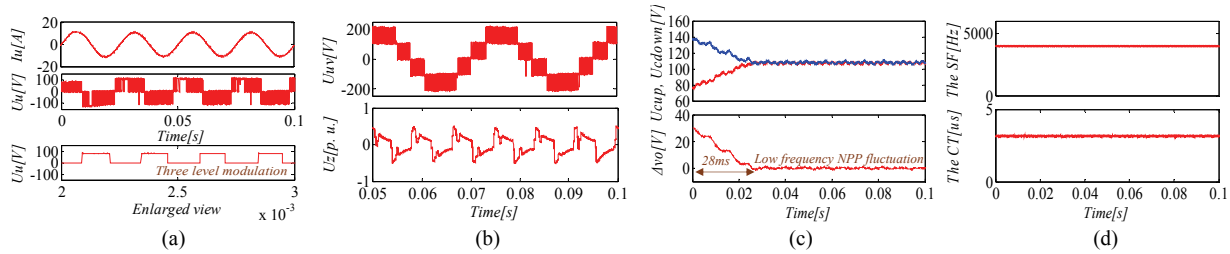

Fig. 18. Conventional NTV-PWM based NPP control (OC2): (a) i_u and u_u; (b) u_{uv} and u_z; (c) *NPP*; (d) SF and CT.

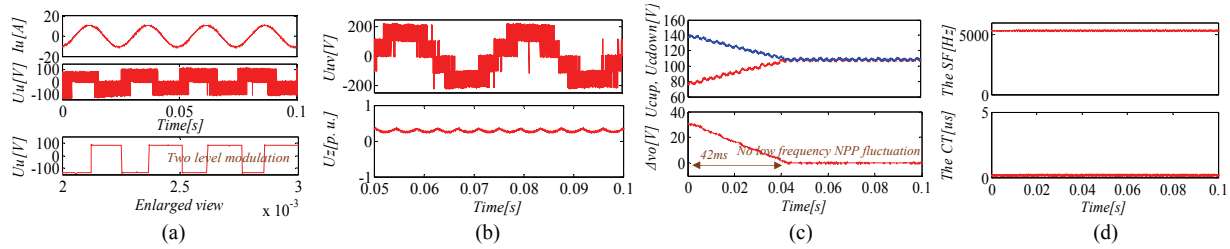

Fig. 19. Conventional DMW method with a compensator (OC2): (a) i_u and u_u; (b) u_{uv} and u_z; (c) *NPP*; (d) SF and CT.

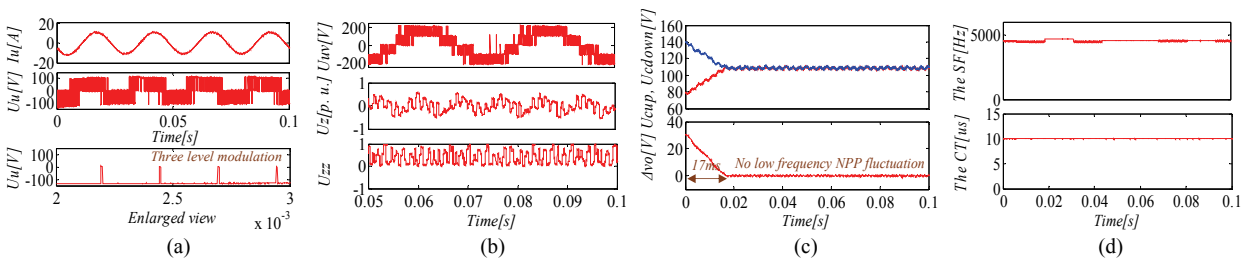

Fig. 20. NPP control based on the search optimization method of 2-DOF (OC2): (a) i_u and u_u; (b) u_{uv}, u_z and u_{zz}; (c) *NPP*; (d) SF and CT.

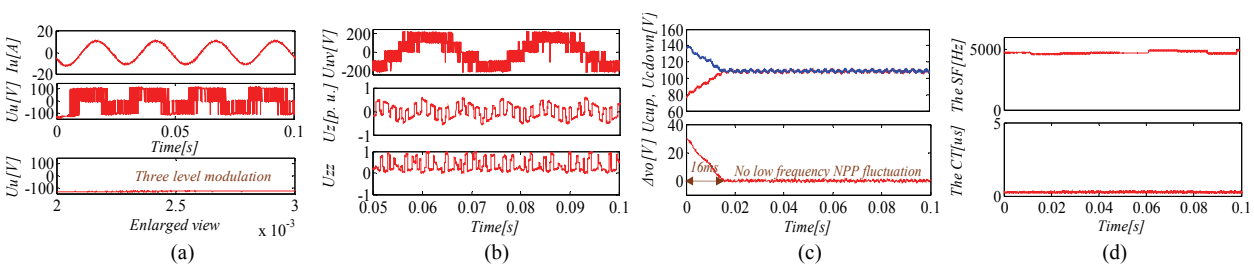

Fig. 21. Proposed direct calculation method of the optimal 2-DOF based NPP control (OC2): (a) i_u and u_u; (b) u_{uv}, u_z and u_{zz}; (c) *NPP*; (d) SF and CT.

TABLE II
EXPERIMENTAL PARAMETERS (OC1)

Methods	*THD (Uuv)*	*SF*	*Low frequency NPP fluctuation*	*NPP drift/ control ability*	*CT*
NTV-PWM based NPP control	37.87%	4.0kHz	×	○/middle	3 us
DWM method	53.78%	5.3kHz	○	○/weak	0.15 us
Search optimization method	54.92%	4.8kHz	○	○/strong	10 us
Proposed direct calculation method	47.63%	4.8kHz	○	○/strong	0.3 us

cannot be overcome. In some medium and high voltage high-power applications, which have an urgent need to reduce the DC-link capacitors, this processing is intolerable.

On the other hand, the DMW method with a compensator can solve the low frequency NPP fluctuation problem. However, this is done at the cost of the THD, SF and NPP drift control capability. When compared with these conventional approaches, the search optimization method and the proposed method can solve the two types of NPP problems simultaneously and have a stronger control capability for the NPP drift problem. Although the output performances of the THD and SF are worse than those of the NTV-PWM, they are improved when compared with the DMW method. More importantly, the proposed method can achieve a more accurate 2-DOF with a lower amount of calculations when compared with the search

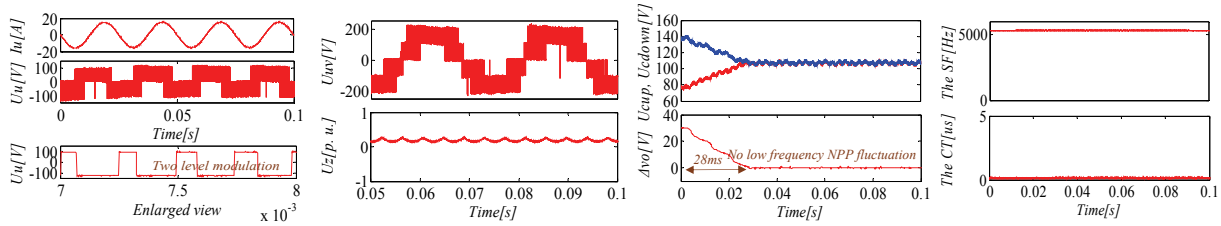

Fig. 22. Conventional DMW method with a compensator (OC3): (a) i_u and u_u; (b) u_{uv} and u_z; (c) *NPP*; (d) SF and CT.

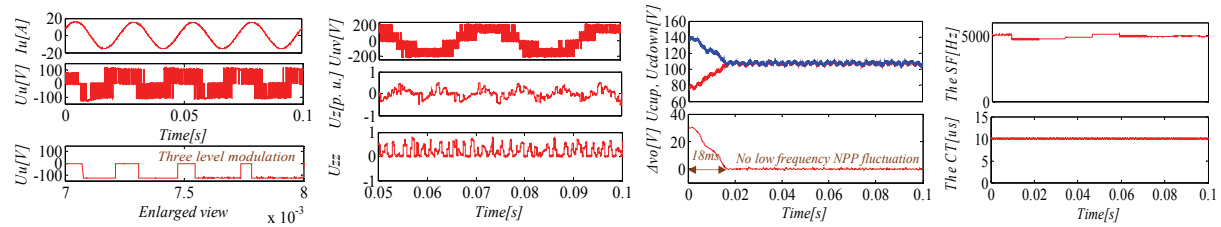

Fig. 23. NPP control based on the search optimization method of 2-DOF (OC3): (a) i_u and u_u; (b) u_{uv}, u_z and u_{zz}; (c) *NPP*; (d) SF and CT.

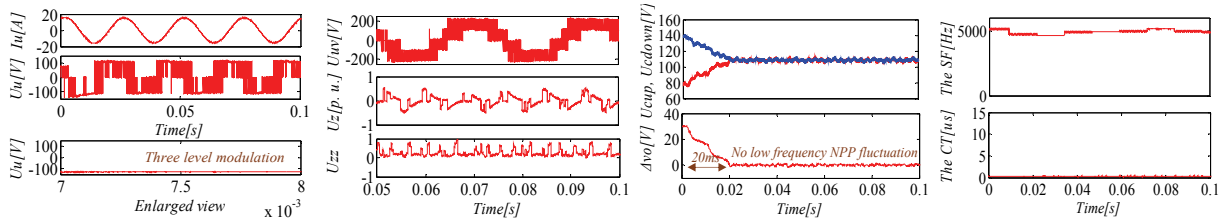

Fig. 24. Proposed direct calculation method of the optimal 2-DOF based NPP control (OC3): (a) i_u and u_u; (b) u_{uv}, u_z and u_{zz}; (c) *NPP*; (d) SF and CT.

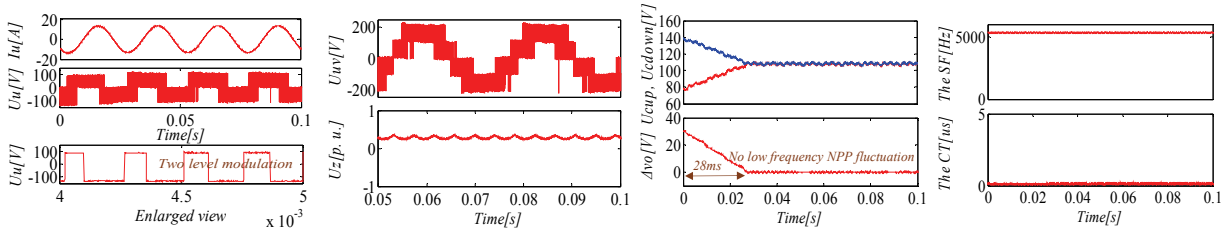

Fig. 25. Conventional DMW method with a compensator (OC4): (a) i_u and u_u; (b) u_{uv} and u_z; (c) *NPP*; (d) SF and CT.

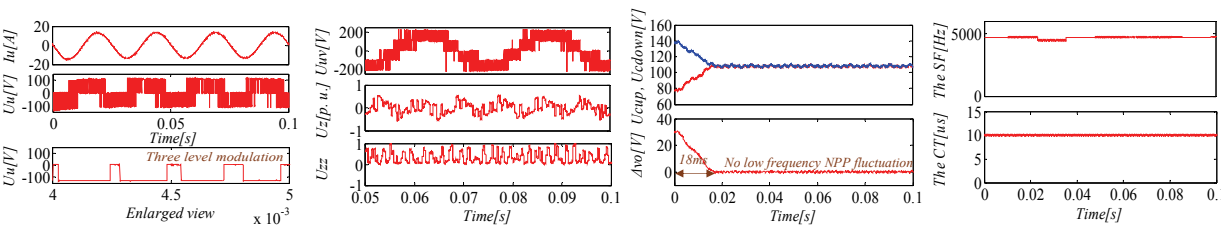

Fig. 26. NPP control based on the search optimization method of 2-DOF (OC4): (a) i_u and u_u; (b) u_{uv}, u_z and u_{zz}; (c) *NPP*; (d) SF and CT.

optimization method, which utilizes the proposed method that is suitable for some industry applications with an in expensive DSP. In fact, the output performance of the THD is also better than that of the search optimization method. It should be noted that the word "optimal" in this paper aims at an optimal NPP control performance, rather than an optimal THD. Theoretically, the THD is determined by the modulation strategies. Therefore, the optimal 2-DOF obtained by the search optimization method cannot ensure that the THD is better than that of the proposed method. It is not possible to realize the search optimization method online with the infinite precision u_z and u_{zz} considering the amount of calculations. Thus, u_z and u_{zz} are divided to 100

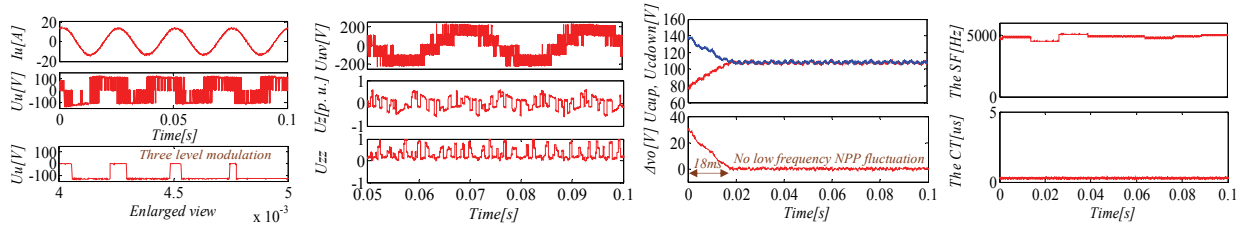

Fig. 27. Proposed direct calculation method of the optimal 2-DOF based NPP control (OC4): (a) i_u and u_u; (b) u_{uv}, u_z and u_{zz}; (c) *NPP*; (d) SF and CT.

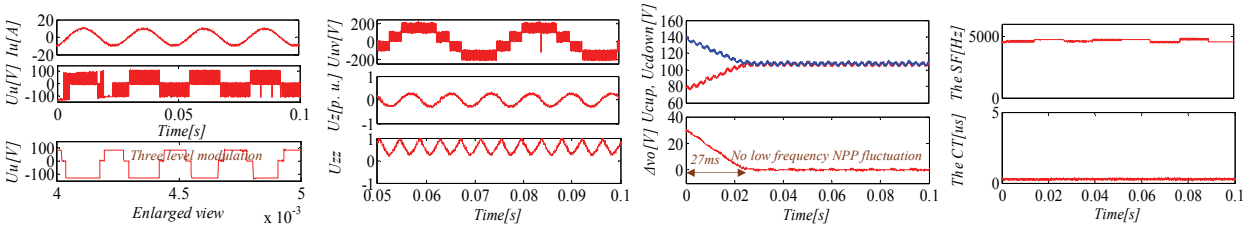

Fig. 28. Proposed direct calculation method of the optimal 2-DOF based NPP control (OC5): (a) i_u and u_u; (b) u_{uv}, u_z and u_{zz}; (c) *NPP*; (d) SF and CT.

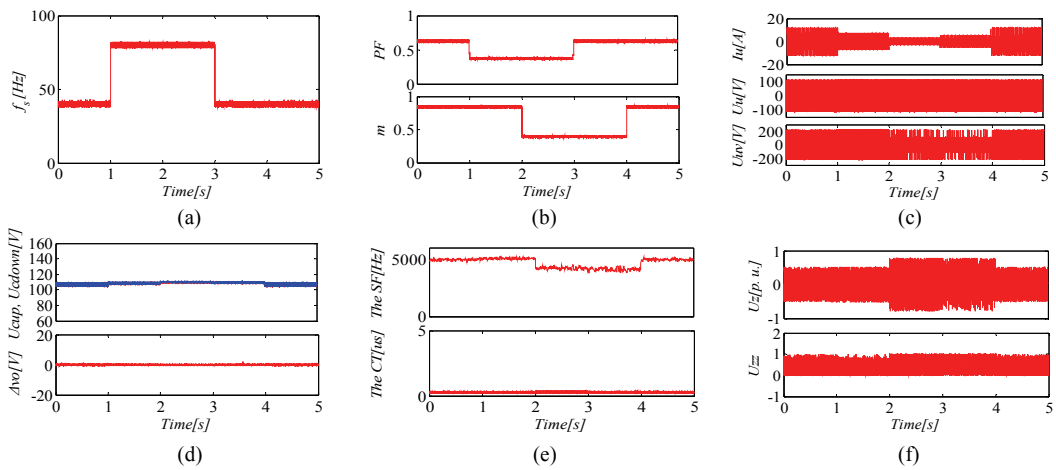

Fig. 29. Proposed direct calculation method of optimal 2-DOF based NPP control (Sudden change loads): (a) Output frequency; (b) PF and m; (c) i_u, u_u ;and u_{uv}; (d) NPP; (e) SF and CT; (f) u_z and u_{zz} .

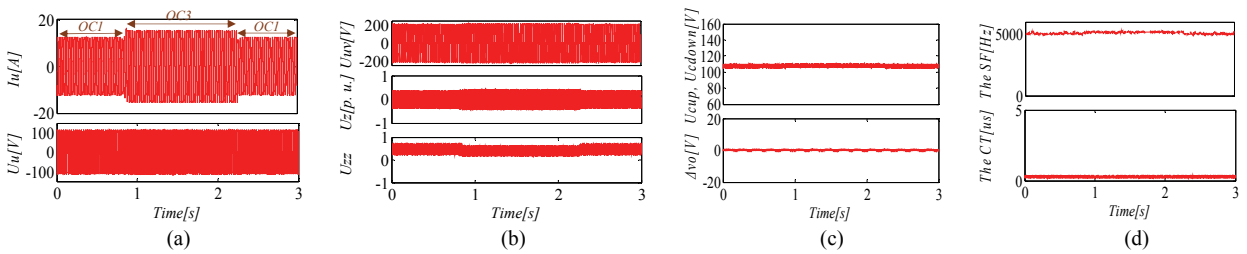

Fig. 30. Proposed direct calculation method of the optimal 2-DOF based NPP control (Sudden change loads): (a) i_u and u_u; (b) u_{uv}, u_z and u_{zz}; (c) *NPP*; (d) SF and CT.

parts and 10 parts in the experiment results, respectively. On the other hand, the proposed method is based on the direct calculation method. Therefore, in theory, the two methods are the same when u_z and u_{zz} have infinite precision. However, this is impossible. Thus, the two methods achieve different optimal 2-DOF. This can also be confirmed from Figs. 16(b) and 17(b). As a result, the THD of the two methods are also different.

Based on an analysis of Figs. 14-17, it can be clearly seen that the proposed method has many advantages over the conventional NPP control. In fact, similar conclusions can also be achieved based on Figs. 18-28. These results show that the proposed method is valid under any operation

TABLE III
A SUMMARY ON THE CHARACTERISTICS OF THREE NPP CONTROLS

Methods	OC1			OC2			OC3			OC4			OC5		
	CS	SF	CT	CS	SF	CT	CS	SF	CT	CS	SF	CT	CS	SF	CT
DWM method	40ms	5.3kHz	0.15us	42ms	5.3kHz	0.15us	28ms	5.3kHz	0.15us	28ms	5.3kHz	0.15us	180ms	5.3kHz	0.15us
Search optimization method	23ms	4.8kHz	10.0us	17ms	4.6kHz	10.0us	18ms	4.8kHz	10.0us	18ms	4.7kHz	10.0us	27ms	4.6kHz	10.0us
Proposed direct calculation method	22ms	4.8kHz	0.30us	16ms	4.7kHz	0.30us	20ms	4.8kHz	0.30us	18ms	4.8kHz	0.30us	27ms	4.6kHz	0.30us

conditions. A summary is given as Table III. Since the NTV-PWM based NPP control cannot deal with the low-frequency NPP fluctuation problem, it is not summarized in Table III. CS is the NPP control speed.

B. NPP Control Performance of the Proposed Method under Sudden Load Changes

Based on the explanations in section IV.A, the validity and feasibility of the proposed method under stable loads have been verified. In this part, some experimental results are also given to show that the proposed method has a good dynamic response under sudden load changes. Since RL loads are utilized in the experiment, the inductive reactance of L can be adjusted by changing the output frequency (f_s). Thus, the PF and phase currents of the RL loads are also changed. Moreover, when the modulation ratio is changed, the phase currents can also be revised. Thus, the operation conditions are set as follows.

1) At 1s, change the output frequency from 40Hz to 80Hz (PF from 0.625 to 0.37, phase current from 8.85A to 5.25A).
2) At 2s, change the modulation ratio from 0.85 to 0.4 (phase current from 5.25A to 2.35A).
3) At 3s, change the output frequency from 80Hz to 40Hz (PF from 0.37 to 0.625, phase current from 2.35A to 3.8A).
4) At 4s, change the modulation ratio from 0.4 to 0.85 (phase current from 3.8A to 8.85A).

It is obvious from Fig. 29 that although the PF, m, phase current and output frequency change abruptly, there is no effects on the NPP control performance of the proposed method. It can maintain the NPP at zero at any point. Moreover, the amount of calculations is also maintained as a low level. Thus, there is no problem with the dynamic response. The NPP control performance of the proposed method is not affected.

Fig. 30 shows experimental results when the operation condition changes from OC1 to OC3 and from OC3 to OC1. Although different RL loads are utilized in OC1 and OC3, there is still no effect on the NPP control performance of the proposed method. It can also verify that the proposed method has a good dynamic response.

V. CONCLUSIONS

In this paper, the low-frequency NPP fluctuation problem for TL-NPC converters is discussed in detail. The DMW method solves this problem by sacrificing the control domains of i_o to keep i_o zero at any time. The search optimization method can adjust the 2-DOF to greatly expand the control domains of i_o. A wider control domain of i_o corresponds to a stronger control capability for coping with the NPP drift problem. In comparison with the DMW method, the SF can also be decreased. However, the calculation amount of the search optimization method is a vital problem for some industrial applications with a cheap DSP. Thus, a direct calculation method is proposed in this paper for achieving the relationships between the NPP and the 2-DOF. The actual optimal 2-DOF can be easily acquired via an interpolation method, which can drastically reduce the calculation amount. Thus, the proposed method realizes the same NPP control performance as the search optimization method but with a small calculation amount, which is vital for some applications with an inexpensive DSP. While maintaining a strong control capability and a fast control speed for the two types of NPP problems, the proposed method can also master the output waveforms, which is beneficial for reducing the SF and improving the EMI problem. In summary, the search optimization method may be the best choice if a high-performance DSP is available, since the principle of the method is easy to understand and apply by general engineering officers. However, if only a low-cost DSP can be used in an application, the method proposed in this paper would be a good choice.

Lastly, it is worth noting that the proposed method is not better than the search optimization method [18], [19] in all aspects, since the relationships between the quasi-optimal and actual optimal values are very complex. Specifically, in this paper, "optimal" only implies that the control performance in the NPP problem is optimal. Thus, the actual optimal 2-DOF may not be the actual optimum, when the THD, SF and NPP problems are considered as a whole. Some further analysis and discussions on the proposed method and the search optimization method will be performed in the future. A careful choice between the two methods should be made based on the specific application.

REFERENCES

[1] A. Nabae, I. Takahashi, and H. Akagi, "A new neutral-point-clamped PWM inverter," *IEEE Trans. Ind. Appl.*, Vol. IA-17, No. 5, pp. 518-523, Sep. 1981.

[2] Z. Ye, Y. Xu, and X. Wu, "A simplified PWM strategy for a neutral-point-clamped (NPC) three-level converter with unbalanced DC links," *IEEE Trans. Power Electron.*, Vol. 31, No. 4, pp. 3227-3238, Apr. 2016.
[3] U. M. Choi, H. H. Lee, and K. B. Lee, "Simple neutral-point voltage control for three-level inverters using a discontinuous pulse width modulation," *IEEE Trans. Energy Convers.*, Vol. 28, No. 2, pp. 434-443, Jun. 2013.
[4] S. R. Pulikanti, M. S. A. Dahidah, and V. G. Agelidis, "Voltage balancing control of three-level active npc converter using SHE-PWM," *IEEE Trans. Power Del.*, Vol. 26, No. 1, pp. 258-267, Jan. 2011.
[5] A. Lewicki, Z. Krzeminski, and H. Abu-Rub, "Space-vector pulsewidth modulation for three-level NPC converter with the neutral point voltage control," *IEEE Trans. Ind. Electron.*, Vol. 58, No. 11, pp. 5076-5086, Nov. 2011.
[6] J. Zaragoza, J. Pou, and S. Ceballos, "A comprehensive study of a hybrid modulation technique for the neutral-point-clamped converter," *IEEE Trans. Ind. Electron.,* Vol. 58, No. 2, pp. 294-304, Feb. 2009.
[7] W. Chenchen, Li. Yongdong, and X. Xi, "A unified SVM algorithm for multilevel converter and analysis of zero sequence voltage components," in *Proc. IECON*, pp. 2020-2024, 2006.
[8] C. Wang and Y. Li, "Analysis and calculation of zero-sequence voltage considering neutral-point potential balancing in three-level NPC converters," *IEEE Trans. Ind. Electron.*, Vol. 57, No. 7, pp. 2262-2271, Jul. 2010.
[9] J. Pou, J. Zaragoza, and S. Ceballos, "A carrier-based PWM strategy with zero-sequence voltage injection for a three-level neutral-point-clamped converter," *IEEE Trans. Power Electron.*, Vol. 27, No. 2, pp. 642-651, Feb. 2012.
[10] S. Busquets-Monge, J. Bordonau, and D. Boroyevich, "The nearest three virtual space vector PWM - a modulation for the comprehensive neutral-point balancing in the three-level NPC inverter," *IEEE Power Electron. Lett.*, Vol. 2, No. 1, pp. 11-15, Mar. 2004.
[11] G. I. Orfanoudakis, M. A. Yuratich, and S. M. Sharkh, "Nearest-vector modulation strategies with minimum amplitude of low-frequency neutral-point voltage oscillations for the neutral-point-clamped converter," *IEEE Trans. Power Electron.*, Vol. 28, No. 10, pp. 4485-4499, Oct. 2013.
[12] W. d. Jiang, S. w. Du, and L. c. Chang, "Hybrid PWM strategy of SVPWM and VSVPWM for NPC three-level voltage-source inverter," *IEEE Trans. Power Electron.*, Vol. 25, No. 10, pp. 2607-2619, Oct. 2010.
[13] S. Busquets Monge, S. Somavilla, and J. Bordonau, "Capacitor voltage balance for the neutral-point-clamped converter using the virtual space vector concept with optimized spectral performance," *IEEE Trans. Power Electron.*, Vol. 22, No. 4, pp. 1128-1135, Jul. 2007.
[14] A. Choudhury, P. Pillay, and S. S. Williamson, "DC-bus voltage balancing algorithm for three-level neutral-point-clamped (NPC) traction inverter drive with modified virtual space vector," *IEEE Trans. Ind. Appl.*, Vol. 52, No. 5, pp. 3958-3967, Sept.-Oct. 2016.
[15] S. Busquets-Monge, J. D. Ortega, and J. Bordonau, "Closed-loop control of a three-phase neutral-point- clamped inverter using an optimized virtual-vector-based pulsewidth modulation," *IEEE Trans. Ind. Electron.*, Vol. 55, No. 5, pp. 2061-2071, May 2008.
[16] J. Zaragoza, J. Pou, and S. Ceballos, "Optimal voltage-balancing compensator in the modulation of a neutral-point-clamped converter," in *Proc. ISIE*, pp. 719-724, 2007.
[17] J. Pou, J. Zaragoza, and P. Rodriguez, "Fast-processing modulation strategy for the neutral-point-clamped converter with total elimination of low-frequency voltage oscillations in the neutral point," *IEEE Trans. Ind. Electron.*, Vol. 54, No. 4, pp. 2288-2294, Aug. 2007.
[18] B. Guan and S. Doki, "A novel neutral point potential balance control of three-level converters based on the search optimization method of dual degrees of freedom," in *Proc. ECCE Europe*, pp. 1-9, 2017.
[19] B. Guan and S. Doki, "A neutral point potential control for three-level neutral-point-clamped converters based on the search optimization method of the two degrees of freedom," *IEEJ Trans. Electr. Electron. Eng.*, Vol. 13, No. 8, pp. 1195-1207, Jul. 2018.

Bo Guan was born in Chengdu, China, in 1989. He received his B.S. and M.S. degrees in Electrical Engineering from Beijing Jiaotong University, Beijing, China, in 2012 and 2015, respectively. He received his Ph.D. degree in Electrical Engineering and Computer Science from Nagoya University, Nagoya, Japan, in 2018. Since 2018, Dr. Guan has been working as an Assistant Professor at Chongqing University, Chongqing, China. His current research interests include multilevel converters, modulation technology, motor driving, etc.

Shinji Doki was born in Nagoya, Japan, in 1966. He received his B.S., M.S. and Ph.D. degrees in Electronic Mechanical Engineering from Nagoya University, Nagoya, Japan, in 1990, 1992 and 1995, respectively. Since 2012, he has been working as a Professor at Nagoya University. His current research interests include control, modeling and signal processing and its application to motor drive systems. Dr. Doki was a recipient of an IEEE Industrial Electronics Society 1992 Best Paper Award as well as paper awards from the FANUC FA and Robot Foundation and the Institute of Electrical Engineers of Japan.